Measurement of the angular distribution of γ-rays after neutron capture by ^{139}La for a T-violation search

Takuya Okudaira[1,a], *Hirohiko M.* Shimizu[2], *Masaaki* Kitaguchi[3], *Katsuya* Hirota[2], *Christopher C.* Haddock[4], *Ikuya* Ito[2], *Tomoki* Yamamoto[2], *Shunsuke* Endo[2], *Kohei* Ishizaki[2], *Takumi* Sato[2], *Shusuke* Takada[5], *Jun* Koga[5], *Tamaki* Yoshioka[6], *Takashi* Ino[7], *Kouichiro* Asahi[8], *Takamasa* Momose[9], *Takahiro* Iwata[10], *Takayuki* Oku[1], *Kenji* Sakai[1], *Atsushi* Kimura[11], *Taro* Nakao[11], *Masanori* Hino[12], *Tatsushi* Shima[13], and *Yutaka* Yamagata[14]

[1] J-PARC center, Japan Atomic Energy Agency, Tokai, Ibaraki 319–1184, Japan
[2] Department of Physics, Nagoya University, Furocho, Chikusa, Nagoya, Aichi 464–8601, Japan
[3] Kobayashi-Maskawa Institute, Nagoya University, Furocho, Chikusa, Nagoya, Aichi 464–8601, Japan
[4] National Institute of Standards and Technology, 100 Bureau Dr, Gaithersburg, MD 20899, USA
[5] Department of Physics, Kyushu University, 744 Motooka, Nishi, Fukuoka, Fukuoka 819–0395, Japan
[6] Research Center of Advanced Particle Physics, Kyushu University, 744 Motooka, Nishi, Fukuoka, Fukuoka 819–0395, Japan
[7] Institute of Material Structure Science, High Energy Accelerator Organization (KEK), Oho 1–1, Tsukuba, Ibaraki 305–0801, Japan
[8] Department of Physics, Tokyo Institute of Technology, 2-12-1 Oh-okayama, Meguro, Tokyo 152–8551, Japan
[9] Department of Chemistry, UBC Faculty of Science, University of British Columbia, Vancouver, British Columbia V6R1Z1, Canada
[10] Department of Earth and Environmental Sciences, Yamagata University, 1-4-12 Kojirakawa, Yamagata 990–8560, Japan
[11] Nuclear Science and Engineering Directorate, Japan Atomic Energy Agency, Japan
[12] Research Reactor Institute, Kyoto University, 2 Asashiro-nishi, Kumatoricho, Senngan-gun, Osaka 590–0494, Japan
[13] Research Center for Nuclear Physics, Osaka University, 10–1 Mihogaoka, ibaraki, Osaka 567–0047, Japan
[14] RIKEN Center for Advanced Photonics, RIKEN, Hirosawa 2–1, Wako, Saitama 351–0198, Japan

Abstract. Parity violating effects enhanced by up to 10^6 times compared to proton-proton scattering have been observed in several neutron capture induced compound nuclei. This enhancement is explained as an interference between an s-wave and a p-wave amplitude (s-p mixing). Theory predicts that this mechanism can also enhance T-violating effects. For estimation of this enhancement in a promising candidate nucleus, we measured the angular distribution of γ-rays in the (n, γ) reaction induced in a ^{139}La target. Experiments were performed at J-PARC, using a germanium detector array at an intense neutron beam. Analysis of the observed angular dependence around the 0.74 eV p-wave resonance allowed us to determine the ratio of the partial p-wave neutron width to the total neutron width in the entrance channel of the compound nucleus. We also report our development of a ^{3}He spin filter needed as an epithermal-neutron polarizer for the T-violation search.

1. Strategy to search for T-violation in compound nuclei

It is well known that the weak interaction violates parity symmetry. Tiny parity violation caused by the hadronic weak interaction is observed as a helicity dependence of the cross section of p-p scattering in experiments using a polarized proton beam and an unpolarized proton target, and the size of this fundamental parity violating asymmetry is approximately 10^{-7} [1–3].

Very large parity violating asymmetries with a size of 10^{-1} at maximum have been observed in several compound nuclei formed after neutron capture by stable nuclides such as ^{139}La, ^{131}Xe, and ^{81}Br (Fig. 1). The parity violation was measured as a longitudinal asymmetry of the neutron capture cross section, A_{L}. This parity violation occurs in a p-wave resonance (neutron orbital angular momentum $l = 1$) located at the tail of an s-wave resonance ($l = 0$). It is theoretically understood that fundamental parity violation enhancement by up to 10^6 is a result of an interference between the s-wave and thee p-wave amplitudes, called "s-p mixing".

There is a theoretical prediction that fundamental CP-violation can be also enhanced in these nuclei under the assumption of being due to the s-p mixing as for the enhancement of P-violation [4]. This implies that, invoking the CPT theorem, time reversal violation is also enhanced in these systems and can be searched for with very sensitive measurements of the compound nucleus system. We are aiming to search for T-violation beyond that predicted by the Standard Model, for which several experiments and developments are in progress at J-PARC.

The forward scattering amplitude of polarized neutrons incident upon polarized nuclei can be written as

$$f = A' + B'\boldsymbol{\sigma} \cdot \hat{\boldsymbol{I}} + C'\boldsymbol{\sigma} \cdot \hat{\boldsymbol{k}} + D'\boldsymbol{\sigma} \cdot (\hat{\boldsymbol{I}} \times \hat{\boldsymbol{k}}), \quad (1)$$

where $\boldsymbol{\sigma}$, $\hat{\boldsymbol{I}}$ and $\hat{\boldsymbol{k}}$ are unit vectors parallel to the spin of the incident neutron, the spin of the target nucleus

[a] e-mail: okudaira@post.j-parc.jp

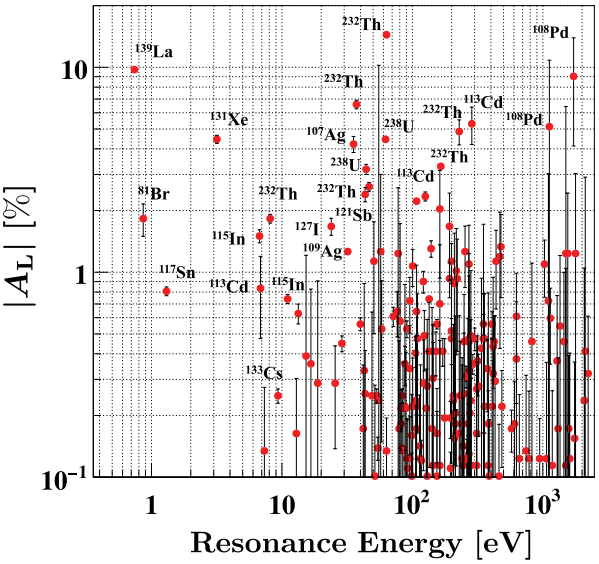

Figure 1. Large enhanced parity violation in several nuclei. The vertical axis is the longitudinal asymmetry of the neutron absorption cross section at a p-wave resonance. The horizontal axis is resonance energy of the p-wave resonance.

and the wave vector of the neutron, respectively [5]. Here we assume that the target nucleus is purely vector polarized. A' is the spin independent (P-even, T-even) term, the imaginary part of which is related to the total neutron cross section via the optical theorem. B' is the spin dependent (P-even, T-even) term corresponding to a "pseudomagnetic" neutron spin rotation through the polarized target. C' is the P-violating (P-odd, T-even) term, which is enhanced for the nuclei mentioned before. The imaginary part of the T-violating (T-odd and P-odd) term D' gives rise to a difference of total cross sections observed in the transmission of neutrons, polarized parallel and anti-parallel to the $\hat{\boldsymbol{I}} \times \hat{\boldsymbol{k}}$ axis:

$$\Delta\sigma_{\mathrm{T}} = \frac{4\pi}{k}\mathrm{Im}(f_+ - f_-) = \kappa(J)\frac{W_{\mathrm{T}}}{W}\Delta\sigma_{\mathrm{P}}. \qquad (2)$$

The expression on the right side relates the T-violating effect to the (enhanced) P-violating cross section difference $\Delta\sigma_{\mathrm{P}}$ measured via transmission of the two neutron helicity states through the unpolarized target (due to the C' term in Eq. (1)). W_{T} and W are the T-violating and P-violating matrix elements (ranges of values for their ratio as predicted by various models can be found in Ref. [4]). The factor $\kappa(J)$ includes amplitudes of the partial neutron widths and depends on the total channel spin $J = I + 1/2$ or $J = I - 1/2$ (I being the spin of the target nucleus). The amplitudes can be expressed in terms of two variables x and y which are given by

$$x^2 = \frac{\Gamma^{\mathrm{n}}_{\mathrm{p},j=\frac{1}{2}}}{\Gamma^{\mathrm{n}}_{\mathrm{p}}}, \quad y^2 = \frac{\Gamma^{\mathrm{n}}_{\mathrm{p},j=\frac{3}{2}}}{\Gamma^{\mathrm{n}}_{\mathrm{p}}}, \qquad (3)$$

where $\Gamma^{\mathrm{n}}_{\mathrm{p}}$ is the neutron width of the p-wave resonance and $\Gamma^{\mathrm{n}}_{\mathrm{p},j=\frac{1}{2}}$ and $\Gamma^{\mathrm{n}}_{\mathrm{p},j=\frac{3}{2}}$ are its partial neutron widths for the two values of total angular momentum j of the neutron. The variables x and y satisfy

$$x^2 + y^2 = 1 \qquad (4)$$

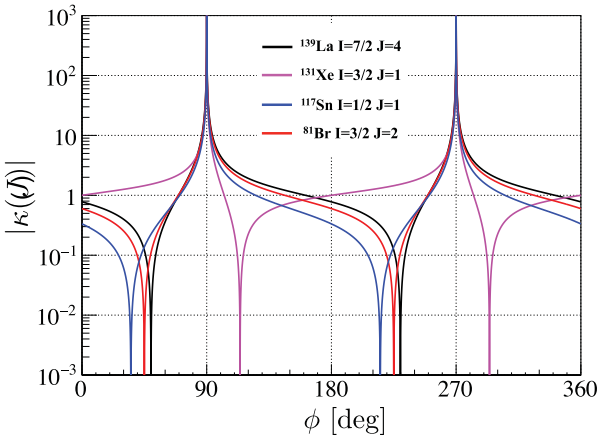

Figure 2. ϕ dependencies of $\kappa(J)$ for the target isotopes ^{139}La, ^{131}Xe, ^{81}Br and ^{117}Sn.

Table 1. Properties of the candidate nuclei for the T-violation search. The nuclear polarization method has not yet been established except for ^{139}La and ^{131}Xe.

	E_{p} [eV]	A_{L} [%]	I	Abundance [%]
^{139}La	0.74	9.8 ± 0.2	7/2	99.91
^{81}Br	0.88	0.77 ± 0.33	3/2	49.31
^{117}Sn	1.33	0.79 ± 0.04	1/2	7.68
^{131}Xe	3.2	4.3 ± 0.2	3/2	21.2

due to the relation $\Gamma^{\mathrm{n}}_{\mathrm{p}} = \Gamma^{\mathrm{n}}_{\mathrm{p},j=\frac{1}{2}} + \Gamma^{\mathrm{n}}_{\mathrm{p},j=\frac{3}{2}}$. A mixing angle ϕ of the $j = 1/2$ and $j = 3/2$ components can then be defined as

$$x = \cos\phi, \quad y = \sin\phi. \qquad (5)$$

For the two channels of total spin, $\kappa(J)$ is given by [6]

$$\kappa(J) = \begin{cases} (-1)^{2I}\left(1 + \frac{1}{2}\sqrt{\frac{2I-1}{I+1}}\frac{y}{x}\right) & (J = I - \frac{1}{2}) \\ (-1)^{2I+1}\frac{I}{I+1}\left(1 - \frac{1}{2}\sqrt{\frac{2I+3}{I}}\frac{y}{x}\right) & (J = I + \frac{1}{2}) \end{cases}. \qquad (6)$$

As examples, ϕ dependencies are shown in Fig. 2 for the target isotopes ^{139}La, ^{131}Xe, ^{81}Br and ^{117}Sn. Eq. (2) and Eq. (6) indicate that the T-violation sensitivity strongly depends on the value of ϕ. Therefore, it is important to determine $\kappa(J)$ for an estimate of the experimental sensitivity.

First of all, we need to find suitable nuclei for the T-violation search. Nuclei that have large $\Delta\sigma_{\mathrm{P}}$ and large $\kappa(J)$ are obviously advantageous. Helpful for a larger statistical sensitivity are a large natural abundance of the nucleus to be employed and a p-wave resonance sitting at low energy where typical neutron sources can provide high beam intensities. Small nuclear spin is also important for the nuclear polarization because nuclei that have large spin are difficult to polarize due to the quadrupole coupling with intra-atomic electric fields, leading to broad lines of magnetic resonance. Unfortunately, the method for the nuclear polarization has not been established for most of the nuclei that otherwise might be suitable. Candidate nuclei for the experiment are ^{139}La, ^{131}Xe, ^{81}Br and ^{117}Sn and others, whose $\Delta\sigma_{\mathrm{P}}$ is large and resonance energy is low. Their properties are shown in Table 1.

The isotope ^{139}La looks particularly promising, also due to its high natural abundance. In addition, an exceptional high nuclear polarization of about 50% has been achieved using a Neodymium doped $LaAlO_3$ crystal at PSI [7]. However, $\kappa(J)$ of these nuclei is still unknown. This can be extracted from measurements of angular distributions of (n,γ) reactions using unpolarized neutrons (see next section). We have recently performed such measurements at J-PARC for the target nuclei ^{139}La, ^{131}Xe, ^{81}Br, ^{117}Sn, ^{115}In, ^{113}Cd, ^{127}I, and ^{103}Rh.

On the other hand, an experiment to verify the compound nuclear model is also ongoing at J-PARC. The enhancement of the P- and T-violation is based on the assumption of the s-p mixing and is derived from the statistical interpretation of the compound nuclear model. It can be tested by measuring the angular distribution of the (n,γ) reaction using polarized neutrons. We have installed a neutron polarizer at a neutron beam line and confirmed that it delivers polarized epithermal neutrons (see Sect. 3 and Ref. [8]).

This paper reports the result of a measurement of $\kappa(J)$ for the target nucleus ^{139}La and the development of a neutron polarizer for the T-violation search. The results of unpolarized (n,γ) measurements for the target nuclei ^{117}Sn and ^{81}Br are discussed in Refs. [9] and [10], respectively. An experiment to measure the (n,γ) reaction using polarized neutrons for verification of the compound nuclear model is reported in Ref. [8].

2. Measurement of the angular distribution in ^{139}La(n,γ) reactions

2.1. Formalism of the angular distribution of γ-rays

In order to obtain the value of $\kappa(J)$, it is necessary to determine ϕ by measuring the angular distribution of γ-rays in (n,γ) reactions. The corresponding differential cross section for unpolarized neutrons and unpolarized nuclei can be written as

$$\frac{d\sigma}{d\Omega} = \frac{1}{2}\left(a_0 + a_1\cos\theta_\gamma + a_3\left(\cos^2\theta_\gamma - \frac{1}{3}\right)\right), \quad (7)$$

where θ_γ is the polar angle of the outgoing γ-ray momentum for the case that only s- and p-wave amplitudes are present [11]. The angular correlation terms a_0, a_1 and a_3 can be written as

$$\begin{aligned} a_0 &= \sum_{r_s}\left|V_{1r_s}\right|^2 + \sum_{r_p}\left|V_{2r_p}\right|^2, \\ a_1 &= 2\,\mathrm{Re}\sum_{r_s r_p j'} V_{1r_s}V^*_{2r_p}P(J_{r_s}J_{r_p}\frac{1}{2}j'1IF)z_{r_p j'}, \\ a_3 &= 3\sqrt{10}\,\mathrm{Re}\sum_{r_p j r'_p j'} V_{2r_p}V^*_{2r'_p} \\ &\quad \times P(J_{r_p}J_{r'_p}jj'2IF)\begin{Bmatrix} 2 & 1 & 1 \\ 0 & \frac{1}{2} & \frac{1}{2} \\ 2 & j & j' \end{Bmatrix} z_{r_p j}z_{r_p j'}, \end{aligned} \quad (8)$$

where

$$\begin{aligned} P(JJ'jj'mIF) &= (-1)^{J+J'+j'+I+F}\frac{3}{2} \\ &\quad \times\sqrt{(2J+1)(2J'+1)} \\ &\quad \times\sqrt{(2j+1)(2j'+1)} \\ &\quad \times\begin{Bmatrix} m & j & j' \\ I & J' & J \end{Bmatrix}\begin{Bmatrix} m & 1 & 1 \\ F & J & J' \end{Bmatrix}. \end{aligned} \quad (9)$$

Here I is the spin of the target nucleus, J and J' are the spin of the compound states, j and j' are the total angular momenta of the incident neutrons, m is an integer number, and F is the spin of the final state. $z_{r_p j}$ is given as

$$z_{r_p j} = \begin{cases} x & (j=\frac{1}{2}) \\ y & (j=\frac{3}{2}) \end{cases}, \quad (10)$$

with x and y as defined in Eq. (3). V_1 and V_2 are s-wave and p-wave amplitudes respectively, written as

$$\begin{aligned} V_{1r_s} &= -\frac{1}{2k}\frac{\sqrt{g_{r_s}\Gamma^{\mathrm{n}}_{r_s}\Gamma^{\gamma}_{r_s f}}}{E_{\mathrm{n}} - E_{r_s} + i\Gamma_{r_s}/2}, \\ V_{2r_p} &= -\frac{1}{2k}\frac{\sqrt{g_{r_p}\Gamma^{\mathrm{n}}_{r_p}\Gamma^{\gamma}_{r_p f}}}{E_{\mathrm{n}} - E_{r_p} + i\Gamma_{r_p}/2}, \end{aligned} \quad (11)$$

where k is the neutron wave number, E_{n} is its kinetic energy, Γ^{n}_r is the neutron width, Γ^{γ}_{rf} is the partial γ width to f-th final state, and E_r is the energy of the neutron resonance. The subscript of r in all quantities indicates whether it is an s- or p-wave, and g_r is statistical weight factor defined as

$$g_r = \frac{2J_r+1}{2(2I+1)}. \quad (12)$$

For further details of this formalism please see Ref. [11]. Since E_{n} dependent functions a_1 and a_3 belonging to specific angular dependences of γ-ray emission depend on x and y, the parameter ϕ (related to x and y via Eq. (5)) can be determined from measurements of the angular distribution of γ-rays.

2.2. Experimental setup

The experiment to measure the angular distribution was conducted at the ANNRI (Accurate Neutron-Nucleus Reaction measurement Instrument) beam line of the Material and Life science experimental Facility (MLF) of the Japan Proton Accelerator Research Complex (J-PARC). A schematic view of the beam line is shown in Fig. 3.

The average proton beam power was 150 kW during the experiment. A beam of pulsed neutrons was provided with a repetition rate of 25 Hz and collimated to a 22 mm diameter at the target position. The total measurement time for the ^{139}La(n,γ) reaction was about 60 hours (5.4×10^6 shots). A $^{\mathrm{nat}}$La target with a dimension of $1\times40\times40\,\mathrm{mm}^3$ was used. The angular distribution was measured with a detector array consisting of 22 germanium crystals (Fig. 4), whose angles are 36°, 71°, 72°, 90°, 108°, 109°, and 144° with respect to the neutron beam

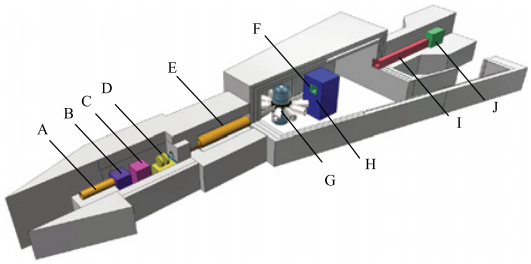

Figure 3. The schematic view of ANNRI beam line [15]. (A) Collimator, (B) T_0-chopper, (C) Neutron filter, (D) Disk chopper, (E) Collimator, (F) Iron, (G) Germanium detector assembly, (H) Concrete, (I) Boron resin, and (J) Beam stopper (Iron).

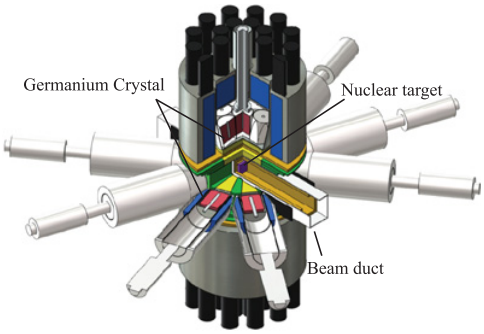

Figure 4. Schematics of the germanium spectrometer at the ANNRI beam line.

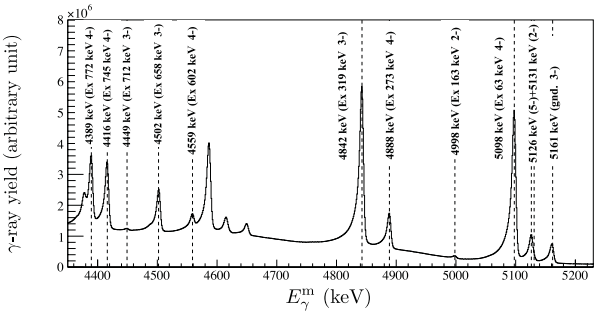

Figure 5. γ-ray spectrum measured with the La target. E_γ corresponds to the energy deposited in the germanium crystals.

line. The nuclear target was mounted in the center of the spectrometer at a distance of 21.5 m from the neutron source. This length determines the baseline for the neutron spectrum via Time-Of-Flight (TOF, see next section). Characteristics and simulation results for this spectrometer are reported in Ref. [16].

2.3. Experimental results

Figure 5 presents a γ-ray energy spectrum displaying intense γ-ray transitions from ^{139}La(n, γ) reactions. Figure 6 shows well-resolved resonances obtained from the γ-ray yield as a function of the neutron TOF. Here, a normalization to the intensity of the incident neutron beam was applied using a TOF spectrum with a ^{10}B target, measuring the 477.6 keV γ-rays from the (resonance-free) ^{10}B(n,$\alpha\gamma$)^{7}Li reaction.

The angular distribution described by Eq. (7) is measured as a function of neutron energy E_n. In our analysis we focus on the 5161 keV γ-rays of the transition

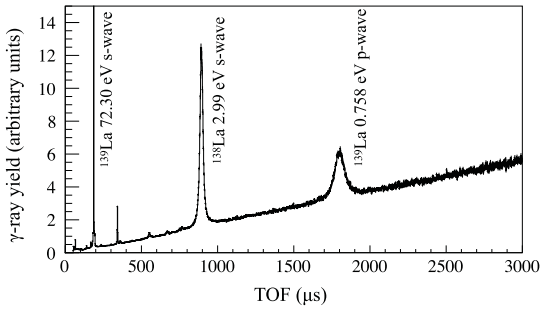

Figure 6. γ-ray yield as function of neutron time of flight measured with the La target.

to the ground state of ^{140}La. While a_0 is the ordinary, symmetric Breit-Wigner function, a_1 is asymmetric around the energy of the p-wave resonance and thus leads, for $\cos\theta_\gamma \neq 0$, to a distortion of the resonance. The sizes of the a_1 and a_3 terms in Eq. (7) depend on the value of ϕ. Accordingly, we can determine ϕ from measurements of the angular distribution of γ-rays as a function of neutron energy in the vicinity of the p-wave resonance. In order to quantify the asymmetric contribution to the shape of the p-wave resonance, we define an asymmetry

$$A_{\mathrm{LH}} = \frac{N_{\mathrm{L}} - N_{\mathrm{H}}}{N_{\mathrm{L}} + N_{\mathrm{H}}}, \tag{13}$$

where N_{L} and N_{H} are the number of events in the regions of $E_{\mathrm{p}} - 2\Gamma_{\mathrm{p}} \leq E_{\mathrm{n}} \leq E_{\mathrm{p}}$ and $E_{\mathrm{p}} \leq E_{\mathrm{n}} \leq E_{\mathrm{p}} + 2\Gamma_{\mathrm{p}}$ of the neutron spectrum, respectively. The peak energy E_{p} and the peak width Γ_{p} of the resonance are obtained from a fit of a Breit-Wigner function convoluted with the pulse structure of the neutron beam and the Doppler broadening due to the thermal motion of target nuclei. The pulse structure of the ANNRI beamline was evaluated in Ref. [13], which to reproduce we adopted an Ikeda-Carpenter function [14]. The thermal motion of the target nuclei has been taken into account using the free-gas model. Figure 7 shows the p-wave resonance gated with the full absorption peak at 5161 keV at the 36° detectors to visualize its asymmetric shape and the definition of N_{L} and N_{H}. The angular distribution of A_{LH} is shown in Fig. 8, and it was fitted with a function $A\cos\theta_\gamma + B$. The fitting results of the parameters A and B were

$$A = -0.388 \pm 0.024, \quad B = -0.075 \pm 0.011. \tag{14}$$

We thus found a clear angular distribution of the γ-rays in the transition from the 0.74 eV p-wave resonance of ^{139}La+n to the ground state of ^{140}La.

From the results, ϕ can be obtained from

$$A = 0.295\cos\phi - 0.345\sin\phi, \tag{15}$$

where the left side is the experimental value of A from Eq. (14), and the right side was obtained from theoretical calculations of a_0 and a_1. Here, the effect of a_3 is neglected. This is justified since a_3 is derived from the p-wave amplitudes which are small compared to the s-wave amplitude. Two solutions were obtained as

$$\phi = (99.2^{+6.3}_{-5.3})^\circ, \quad (161.9^{+5.3}_{-6.3})^\circ. \tag{16}$$

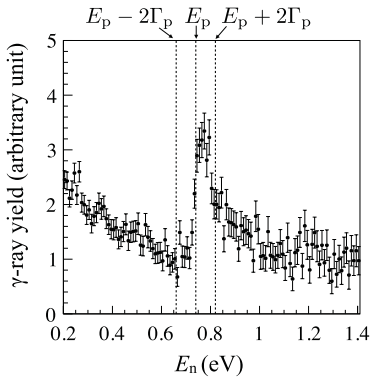

Figure 7. γ-ray yield as function of neutron energy of the p-wave resonance gated with the full absorption peak at 5161 keV at the 36° detectors. The dashed lines describe the regions to obtain N_L and N_H (see text).

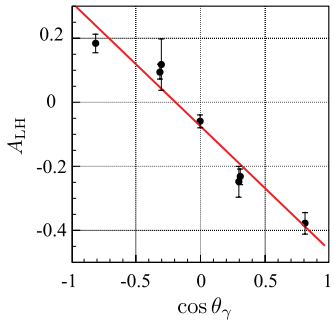

Figure 8. Angular distribution of A_{LH} as defined in Eq. (13). The red line is a linear fit to the measured values (black points).

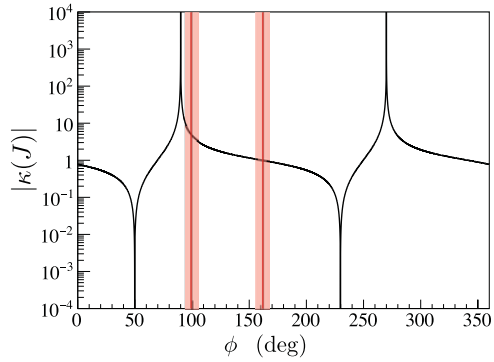

Figure 9. Value of $|\kappa(J)|$ as a function of ϕ. Each solid line and shaded area shows the central value of a solution for ϕ and its 1σ uncertainty, respectively.

Finally, the value of $\kappa(J)$ corresponding to the ϕ solutions is determined as

$$\kappa(J) = 4.84^{+5.58}_{-1.69}, \quad 0.99^{+0.08}_{-0.07}, \tag{17}$$

as visualized in Fig. 9.

This result implies that for ^{139}La target nuclei any fundamental T-violation will be enhanced at a similar or slightly larger level than the P-violation. The details of this experiment and analysis are reported in Ref. [15].

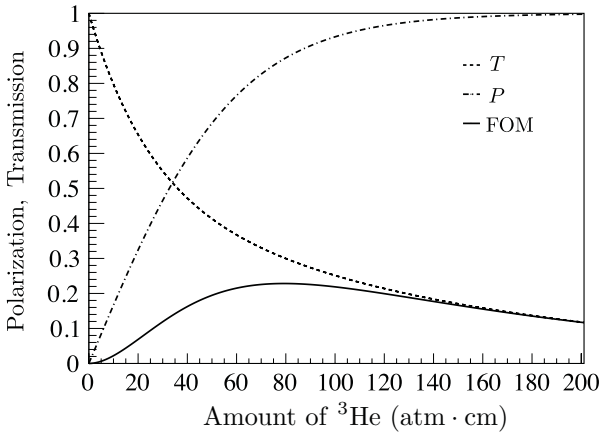

Figure 10. The variation of the neutron polarization, transmission, and FOM as a function of the amount of ^{3}He for 0.74 eV neutrons, evaluated for a ^{3}He polarization of 70%.

Figure 11. Vacuum system for confinement of ^{3}He and Rb in the glass cell of the spin filter.

3. Development of ^{3}He spin filters at JAEA

As discussed in the previous section, the enhancement of T-violation in the 0.74 eV p-wave resonance in ^{139}La+n can be expected to be of similar size as the P-violation. It is however also important to validate the underlying compound nucleus model at this neutron energy, which requires a polarizer for epithermal neutrons. Here the current status of a development of the ^{3}He spin filters at J-PARC is reported.

Polarized ^{3}He has previously been used for polarization of epithermal neutrons at 0.74 eV experiments on P-violation in neutron transmission through a ^{139}La target [17]. The isotope ^{3}He has a very large absorption cross section (10666 barn at thermal energy) for neutrons with spin antiparallel to the ^{3}He spin, while the absorption cross section for parallel neutrons is approximately zero. The neutron beam is polarized passing through a glass cell into which polarized ^{3}He is encapsulated. A figure of merit (FOM) used to describe the polarization efficiency of the

Figure 12. A first ^{3}He spin filter fabricated at J-PARC.

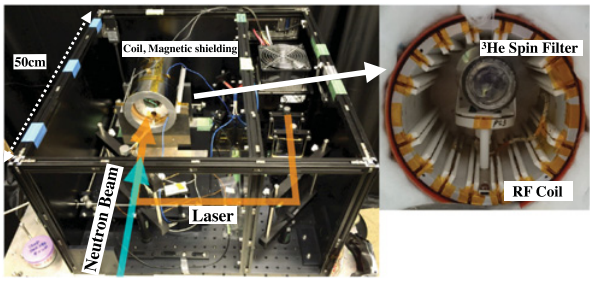

Figure 13. The laser system which can be installed at the neutron beam line. The RF coil is used to flip the polarization of ^{3}He using the NMR method of adiabatic fast passage (AFP).

^{3}He spin filter is defined as

$$\mathrm{FOM} = P^2 T, \tag{18}$$

where P and T are neutron polarization and neutron transmission, respectively. As shown in Fig. 10, P, T and thus the FOM depends on the thickness of the ^{3}He, given by the product of the pressure of ^{3}He gas and the length of the ^{3}He spin filter. For a ^{3}He polarization of 70% and 0.74 eV neutrons, the FOM has a maximum at 79 atm · cm, for which $P = 87\%$ and $T = 30\%$. A development of a large spin filter for epithermal neutrons is ongoing at J-PARC, KEK and Nagoya University.

The glass cell of the ^{3}He spin filter is made from the special, boron-free glass GE180. The cell contains, besides the ^{3}He, Rb used for the spin exchange optical pumping (SEOP) method [18]. The polarization of ^{3}He is maintained by a uniform magnetic field. It relaxes, however, due to the inhomogeneity of the magnetic field, impurities inside the glass cell, and other effects. To avoid contamination from impurities, the cell must be evacuated and filled using a clean gas handling system. Such a system was recently constructed at J-PARC as shown in Fig. 11. The glassware and the stainless steel tubing were baked out for one week at 400 °C and 200 °C, respectively, and the ultimate achieved vacuum was approximately 2×10^{-7} Pa after the baking. A first ^{3}He spin filter fabricated at J-PARC using this vacuum system is shown in Fig. 12. The laser system developed at J-PARC is shown in Fig. 13. It can be installed on the neutron beam line and maintain the ^{3}He polarization during experiments. The laser power is 40 W. A Volume Holographic Grating (VHG) is used for preparation of a narrow range of wavelengths about 795 nm for resonant absorption by the Rb atoms. Since a magnetic field homogeneity at the order of 10^{-4} cm^{-1} is required to prevent decay of the ^{3}He polarization, a homogeneous magnetic field (2 mT) is applied to the ^{3}He spin filter using a coil and a double magnetic shielding. The amount of ^{3}He gas is 15 atm · cm, and 70% ^{3}He polarization are achieved.

Larger ^{3}He spin filters and a laser system with a higher power of 100 W are currently being developed.

References

[1] J.M. Potter et al., Phys. Rev. Lett. **33**, 1307 (1974)
[2] V. Yuan et al., Phys. Rev. Lett. **57**, 1680 (1986)
[3] E.G. Adelberger, W.C. Haxton, Ann. Rev. Nucl. Part. Sci. **35**, 501 (1985)
[4] V.P. Gudkov, Phys. Rep. **212**, 77 (1992)
[5] P.K. Kabir, Phys. Rev. D **37**, 1856 (1988)
[6] V.P. Gudkov, H.M. Shimizu, Phys. Rev. C **97**, 065502 (2018)
[7] P. Hautle, M. Iinuma, Nucl. Instrum. Meth. A **440**, 638 (2000)
[8] T. Yamamoto et al., EPJ Web of Conf. **219**, 09002 (2019)
[9] J. Koga et al., EPJ Web of Conf. **219**, 09004 (2019)
[10] S. Endo et al., EPJ Web of Conf. **219**, 09003 (2019)
[11] V.V. Flambaum, O.P. Sushkov, Nucl. Phys. A **435**, 352–380 (1985)
[12] V.P. Alfimenkov et al., Nucl. Phys. A **398**, 93 (1983)
[13] K. Kino et al., Nucl. Instrum. Meth. A **626**, 58 (2011)
[14] S. Ikeda, J.M. Carpenter, Nucl. Instrum. Methods A, **239**, 536 (1985)
[15] T. Okudaira et al., Phys. Rev. C **97**, 034622 (2018)
[16] S. Takada et al., J. Instrum. **13**, P02018 (2018)
[17] W. Heil et al., Physica B **267–268** 289 (1999)
[18] M.A. Bouchiat et al., Phys. Rev. Lett. **5**, 373 (1960)